

Starbursts and the Butcher-Oemler effect in galaxy clusters

B.M. Poggianti^{1,2} and G. Barbaro¹

¹ Dipartimento di Astronomia, vicolo dell'Osservatorio 5, 35122 Padova, Italy, barbaro@astrpd.pd.astro.it

² Kapteyn Instituut, P.O. Box 800, 9700 AV Groningen, The Netherlands, bianca@astro.rug.nl

Received; accepted

Abstract. In order to explain the spectroscopic observations of most of the galaxies in intermediate redshift clusters, bursts of star formation superimposed to the traditional scenario of galactic evolution are needed.

The analysis of spectral lines and colours by means of an evolutionary synthesis model, including both the stellar contribution and the emission of the ionized gas, allows in most of the cases the determination of the time elapsed since the end of the burst and the fraction of galactic mass involved in it. In the four clusters considered (AC103, AC114, AC118 at $z = 0.31$ and Cl1358+6245 at $z = 0.33$), the theoretical analysis demonstrates that the bursts affect substantial galactic mass fractions, typically 30 % or more.

The observations can be equally well reproduced by either elliptical+burst models or by spiral+burst models in which the star formation is truncated at the end of the burst. A way to determine the galactic original type is suggested.

Key words: galaxies: clusters: general – galaxies: evolution – galaxies: starburst – galaxies: stellar content – HII regions

1. Introduction

Butcher & Oemler (1978, 1984) first showed that the fraction of blue galaxies in rich compact clusters at intermediate redshift ($z < 0.55$) is larger than in similar local ones. The galaxies responsible for this phenomenon, commonly referred to as Butcher-Oemler (BO) effect, were tentatively identified by Butcher and Oemler as normal spirals, subsequently evolving into S0 galaxies due to the depletion of gas in star forming processes. Further works have confirmed the reality of this phenomenon (Couch &

Newell 1984; Dressler et al. 1985; Lavery & Henry 1986, 1988, 1994; Couch & Sharples 1987 (CS87); MacLaren et al. 1988; Mellier et al. 1988; Soucail et al. 1988; Dressler & Gunn 1992; Rakos & Schombert 1995). Especially spectroscopic observations have made a fundamental contribution to its understanding by achieving three main conclusions:

a) the membership of the majority of blue objects has been demonstrated through the determination of their redshift;

b) only in some cases the blue galaxies of the spectroscopic sample have spectra of normal spirals; generally the blue component exhibits four different types of spectra: 1) spectra with emission lines (in particular the line $[\text{OII}]\lambda 3727$) and with absorption Balmer lines of moderate intensity: these spectra are similar to those of local spirals; 2) spectra with strong emission lines and with Balmer absorption lines almost filled in by the emission of the ionized gas in HII regions: these features typify starburst galaxies; 3) spectra with emission lines characteristic of galaxies hosting an AGN; 4) spectra lacking emission lines and with strong absorption Balmer lines: these spectra do not correspond to any normal galaxy of the Hubble sequence. The relative fraction of blue galaxies belonging to the four types is different from cluster to cluster: in some of them the AGNs are in excess (3C295, $z = 0.46$; Dressler and Gunn 1983) in others the blue population is dominated by normal spirals (0024+1654, $z = 0.39$; Dressler et al. 1985). However in most cases the largest fraction consists of type 4) spectra.

c) also several “red” galaxies, not responsible for the BO effect, display unexpected spectral features: the absorption Balmer lines are considerably stronger than in the corresponding local galaxies: the normal ellipticals. Such objects have been called E+A galaxies (Gunn & Dressler 1988) since their spectra can be reproduced by summing up the spectrum of an elliptical galaxy and the spectrum of a stellar population dominated by A type stars. Similar anomalies have been also found by means of multicolour intermediate-band photometry. Ellis et al. (1985) and Ma-

cLaren et al. (1988) found in clusters 0016+16 ($z = 0.54$) and Abell 370 ($z = 0.37$) that some galaxies, whose optical colours are similar to normal ellipticals, exhibit an UV excess. Other elements suggesting an anomalous star forming activity are derived from infrared colours (Lilly 1987; Aragón-Salamanca et al. 1991).

Furthermore, high spatial resolution HST observations (Couch et al. 1994 (CESS94); Dressler et al. 1994; Wirth et al. 1994; Oemler et al. 1995) have provided informations about the morphological appearance of the cluster galaxies and about the high occurrence of mergers/interactions.

Observations suggest that a large fraction of galaxies in rich clusters with intermediate redshift are involved in some anomalous type of star formation, in progress or ended in a relatively recent past, unexpected on the basis of the present knowledge of galaxy evolution. The hypothesis that bursts of star formation could be responsible for all the summarized phenomenology has been analysed in a series of papers (Dressler & Gunn 1982, 1983; Couch & Sharples 1987; MacLaren et al. 1988; Pickles & van der Kruit 1988, 1991; Newberry et al. 1990; Jablonka et al. 1990; Aragón-Salamanca et al. 1991; Charlot & Silk 1994; Barbaro & Poggianti 1995a; Poggianti & Barbaro 1994, 1995; Jablonka & Alloin 1995; Belloni et al. 1995). The alternative possibility of truncation of the star formation in late type galaxies has been also explored in some of the previous papers but such hypothesis seems unable to account for all the variety of the observed facts.

In most cases the theoretical analyses consider only few observable quantities and, in particular, no model presents synthetic estimates of the emission lines due to the gas ionized by hot young stars in HII regions (only CS87 consider the emission-filling of the $H\delta$ line, the emission of the gas being extracted from the spectrum of a spiral galaxy). Consequently the analysis has been mainly restricted to post-starburst objects. Moreover the clusters have been generally studied with different observational techniques (photometric and spectroscopic) and this hinders the intercomparison of the results.

The aim of this work is to derive a theoretical picture which allows the modelling of spectral characteristics and colour indexes and at the same time can be a support for correlating the observational quantities. The tool of this analysis is a spectrophotometric model able to synthesize the integrated spectrum of a galaxy by taking into account the stellar contribution and the emission of the ionized gas. The model allows the computation of the Balmer lines (including the stellar absorption and the gaseous emission) and the principal emission metallic lines such as $[OII]\lambda 3727$. This analysis can shed some light on the nature of the galaxies connected to the BO effect, their original morphological type, their further evolution and therefore their local equivalents. Moreover, since the idea of the bursts of star formation presently seems to be the most reasonable working hypothesis, we want to make a systematic analysis of all the parameters to it connected,

namely the rate of star formation, the duration of the burst and the amount of gas involved.

In this work the analysis is done for a distance and an age corresponding to $z = 0.31$ which is the redshift of three clusters studied in detail by CS87 and also the approximate redshift of the cluster Cl1358+6245 (Fabricant et al. 1991) to which our considerations will be applied.

2. The spectrophotometric model

While a detailed description of the spectrophotometric model is deferred to a further paper (Barbaro & Poggianti 1996, Paper II) here we present only the basic elements which can be useful to critically understand the conclusions.

- The stellar spectrum is computed with an improved version of Barbaro and Olivi's model (1986, 1989) which includes all the stellar advanced evolutionary phases, up to the post-AGB, and takes into account stellar population of different metallicities according to a simple model of chemical evolution. Changes are introduced in the treatment of stellar atmospheres by: a) using Kurucz's new models in the 1993 version, b) employing the library of Jacoby et al. (1984) when a larger resolution was required, as in the case of the synthesis of the Balmer lines (it must be remarked that such spectra have solar metallicity and therefore they should not be proper for modelling metallicity-dependent features in metal-poor populations), c) extending the computation to the infrared regions with Kurucz's models for stars with $T_{\text{eff}} > 5500$ K and the library of observed spectra of Lançon-Rocca Volmerange (1992, LRV) for stars with lower temperatures.

- The gaseous non thermal emission and the dust emission are ignored. Also the dust extinction, which is important in late type galaxies, is not considered: we have preferred to omit the correction instead of using the standard extinction curve of our galaxy, since we completely ignore the dust properties in distant galaxies.

- The emission of the ionized gas is derived by modelling the galaxy spectrum as a superposition of the spectra of HII regions, each of them being excited by a single stellar cluster. It is assumed that such HII regions do not overlap, which is reasonable provided that the star formation rate is not exceedingly high.

- There must be coherence between the stellar and the gaseous spectrum in the sense that the UV photon flux must be derived from the same stars responsible for the stellar emission; this requirement is satisfied by fixing the absolute V magnitude and corresponds to determine the values of the normalization constants in the stellar distribution function.

- In deriving the flux of the metallic lines, the integrated spectrum is approximated with the spectrum of a single equivalent star with appropriate temperature and luminosity equal to the integrated luminosity of the cluster. The validity of this approximation has been confirmed

through a test performed with the photoionization code Cloudy (Ferland 1991), by comparing the results of the integrated spectrum with those of the equivalent star. It was concluded that the results are correct within the uncertainties intrinsic to the evaluation of the lines intensities. These have been derived from Stasinska's models (1990); the inspection of Stasinska's tables shows that the ratios of the lines intensities are generally functions both of the temperature and of the luminosity of the exciting source. In particular this is not true for the ratios of the Balmer lines which practically depend only on the temperature.

- The first eight lines of the Balmer series, the Ly α line and several metallic lines have been synthesized; only the H δ and the [OII] $\lambda 3727$ lines have been considered in the present work.

From the computed spectra several colour indexes in different photometric systems have been derived: the UBVRIJHK system of Johnson (Johnson's UBVRI and JHK from Bessell & Brett 1988), the (U-685) and (418-685) colours of the Durham system (Couch et al. 1983), the (B_J - R_F) used by CS87 (Couch and Newell 1980), the Kron-Cousin system (Bessell 1986), the *gri* system (Schneider et al. 1983), the (1550 - V) colour, originally defined by Burstein et al. (1988). As in the following we are referring to galaxies with $z = 0.32$ in the observer's frame, the response of the 1550 filter at wavelengths shorter than the lower limit of the computed spectrum (1012 Å in the rest frame and 1335 Å in the observer's frame) has been set equal to 0; this however does not affect at least the qualitative conclusions of our analysis. Moreover the following spectral features have been synthesized: D₄₀₀₀, EW([OII]) of the line at $\lambda = 3727$ Å and the intensities of the H α , H β , H δ lines (including absorption and emission components).

Although observations for these quantities are not yet available for the clusters here considered, results concerning D₄₀₀₀ are included because of the equivalence between this index and the colour (B_J - R_F) at $z = 0.31$; (U-685) is considered because such colour is available for another cluster (Abell 370, Aragón-Salamanca et al. 1991) and a theoretical analysis can be useful in order to determine the connection between the H δ strong galaxies and the UV-excess phenomenon observed in other clusters.

Model results for the different galactic types are shown in Table 1; the case of a constantly increasing SFR (Extreme case) has also been considered.

3. Models with bursts of star formation

In this and in the following sections we discuss a set of models in which a burst of star formation is added to a model galaxy of a given morphological type. We define a "starburst" any normal galaxy in which an episode of star formation is superimposed, regardless of its intensity.

The aim of this analysis is to derive theoretical relations between burst parameters and observable quantities.

Table 1. Model results for different normal Hubble types of age 10.4 Gyr and $z=0.32$. Equivalent width values are given in the rest frame, while the other quantities are referred to the observer's frame. The *Ext.* model represents a galaxy whose SFR increases steadily during the evolution

Type	D ₄₀₀₀	(1550 - V)	(B _J - R _F)	EW(H δ)	EW([OII])
E	2.15	4.45	2.67	0.7	0.1
Sa	1.67	-0.87	2.10	1.2	10.0
Sb	1.55	-1.28	1.91	1.2	13.4
Sc	1.44	-1.63	1.69	1.4	16.9
Sd	1.37	-1.79	1.55	1.7	17.6
Ext.	1.28	-2.12	1.30	1.3	21.8

For sake of simplicity the star formation rate during the burst is assumed constant, then the burst is completely characterized by two parameters: 1) the intensity, defined as the ratio ψ_1/ψ_0 of the star formation rate during the burst to the initial SFR, 2) the length Δt . Another important parameter is the time elapsed since the end of the burst $\tau = T - T_f$ where T is the age of the model and T_f is the time at which the burst is ended.

From the previous quantities the fraction of galactic mass that goes into stars during the burst can be derived:

$$\Delta g \propto (\psi_1/\psi_0)\Delta t$$

In the following, unless otherwise stated, Δt and τ are given in million year.

The range of the parameters investigated is wide. 1) the existing observations are barely enlightening on the burst length: local starbursts and mergers seem to suggest timescales larger than usually considered, of the order of Gyr. The following values have been explored: $\Delta t = 1, 10, 100, 500, 1000$ Myr. 2) We want to consider both the case in which the mass involved in the burst is comparable with the galaxy mass (which should mimic a merging episode) and the case in which the gas consumed is internal to the galaxy, in which case its mass is relatively small in respect to the galaxy mass. Consequently the burst intensity is chosen in order to account for a mass of stars formed equal to $10^{-6} - 100$ % of the total mass. 3) The burst evolution is followed from its beginning up to 2 Gyr after its end with the care of analysing in detail the phases during which some observable changes more quickly and therefore we have considered the following times: $\tau = 0, 1, 10, 30, 100, 500, 1000, 2000$ Myr.

An age of 10.4 Gyr, corresponding to a redshift of 0.32, has been adopted for the models. The relation between redshift and age has been derived from a cosmological model of a universe energetically dominated from non-relativistic matter with $q_0 = 0.225$ and $H_0 = 50 \text{ Km s}^{-1} \text{ Mpc}^{-1}$, in which the age of the universe is 15 Gyr. The colours derived by convolution of the model

spectrum with the filter response functions are referred to the observer's frame; however the equivalent widths are computed in the rest frame. The usual convention has been adopted that the equivalent width of the $H\delta$ line is positive for the absorption line and negative for the emission line.

4. Bursts in elliptical galaxies

The star formation rate (SFR) of the underlying galaxy is described by an exponential function with timescale τ_G of 1 Gyr: $\psi = \psi_o \exp(-t/\tau_G)$; the average metal abundance is solar.

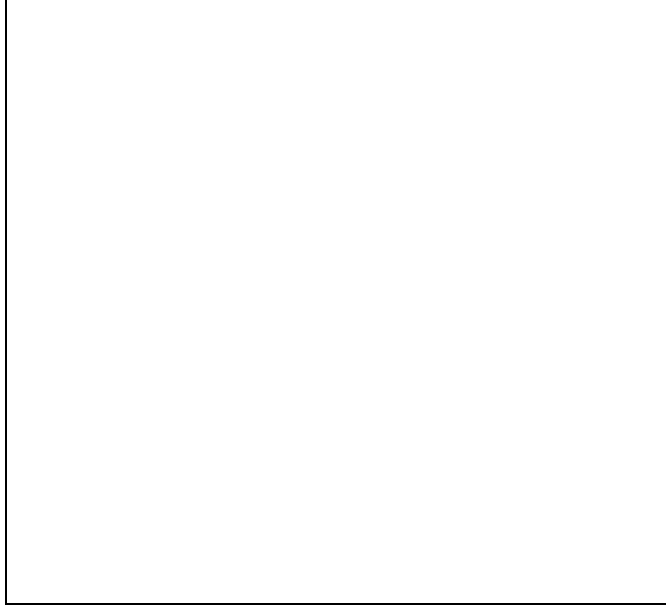


Fig. 1. Model spectra of an unperturbed elliptical (top spectrum) and an elliptical with a burst at three different stages of the evolution (from top to bottom): when the burst is still active; for $\tau = 10$ Myr; for $\tau = 0.5$ Gyr. All the models are computed for an age of 10.4 Gyr. Fluxes are in arbitrary units

In Fig. 1 the evolution of the spectrum is presented when a burst with $\Delta t = 1$ Gyr and $\Delta g = 0.05$ is added to an elliptical galaxy. This case could be considered as representative of a general situation. The metallic lines have been computed, but are not shown because they would require a change in the scale and moreover they are not relevant for the purpose of this figure. From top to bottom are presented: 1) the spectrum of the unperturbed galaxy, 2) the spectrum just at the end of the burst: the $H\alpha$, $H\beta$ emission lines are evident while the $H\delta$ line is emission-filled. The equivalent width of the $[OII]\lambda 3727$ line is equal to 23 Å. From the shape of the continuum and the intensity of the lines this spectrum would be classified as starburst, 3) the spectrum 10 Myr after the end of the burst; the $H\delta$ line with $EW \simeq 3.5$ Å is clearly evident while the

emission lines are now fainter ($EW([OII])=3$), because the remaining hot young stars, although numerous, contribute to the UV flux much less than the massive stars already evolved out of the main sequence. With these features an observed spectrum would be classified as “blue $H\delta$ strong”, 4) the spectrum 0.5 Gyr after the end: the only signatures of the burst are the strong absorption Balmer lines, while emission lines are absent. An object with such a spectrum would be considered as “red $H\delta$ strong”.

The time evolution of some observables after the end of the burst is shown in Fig. 2 for models with $\Delta t = 500$ and different values of ψ_1/ψ_o . In panel a) the behaviour of the equivalent width of the $H\delta$ line is presented: “strong” values ($EW \geq 3$ Å), following the terminology of CS87, are reached only if the mass used in the burst is larger than 2.5 % of the total mass of the galaxy: the curve with full circles corresponds to this limit and this result is independent of the particular choice of Δt . The length of the “strong” phase is a function of Δg and varies between 100 and 1500 Myr: this last value is an upper limit since it corresponds to the lifetime of the stars responsible for the maximum absorption. The time required to reach the maximum is of the order of 10 Myr, independent of the mass implied, and is the time necessary for the emission of the gas to become negligible compared with the absorption.

After the end of the strongest bursts ($\Delta g > 0.5$) for the first millions of years the $H\delta$ line is in emission (according to the adopted convention the EW is negative). Such behaviour does not appear in any of the models with a normal star formation rate (without burst) and therefore is an unambiguous symptom of a burst still in progress or ended by less than 5 million years.

Also the $[OII]\lambda 3727$ line evolves quickly, being associated with those stars able to ionize the gas; the phase in which such line can be revealed (when $EW > 1$ Å) is restricted to the burst length and a period of 10 Myr after its end. There is a short time interval during which the presence of the $[OII]\lambda 3727$ emission line and of the $H\delta$ absorption line are detectable on the spectrum. Of course the probability of catching such an event is small.

The other emission features behave in a similar way; the $H\alpha$ line persists in emission for a smaller period than the $[OII]\lambda 3727$ line due to its superposition with the stellar absorption. The $H\beta$ emission is fainter for the same reason and in absorption it shows the same behaviour as the $H\delta$ line.

In Fig. 2b and 2c the evolution of the colour indexes ($B_J - R_F$) and ($U - 685$) are presented for the same models of Fig. 2a. In Fig. 2b the lower horizontal line marks the limit between blue and red galaxies, according to the definition of CS87, while the upper one sets the limit beyond which the bursting galaxy cannot be distinguished from a normal elliptical. The horizontal line in Fig. 2c separates normal ellipticals from those with UV excess, the last ones being defined as those having ($U-685$) bluer by

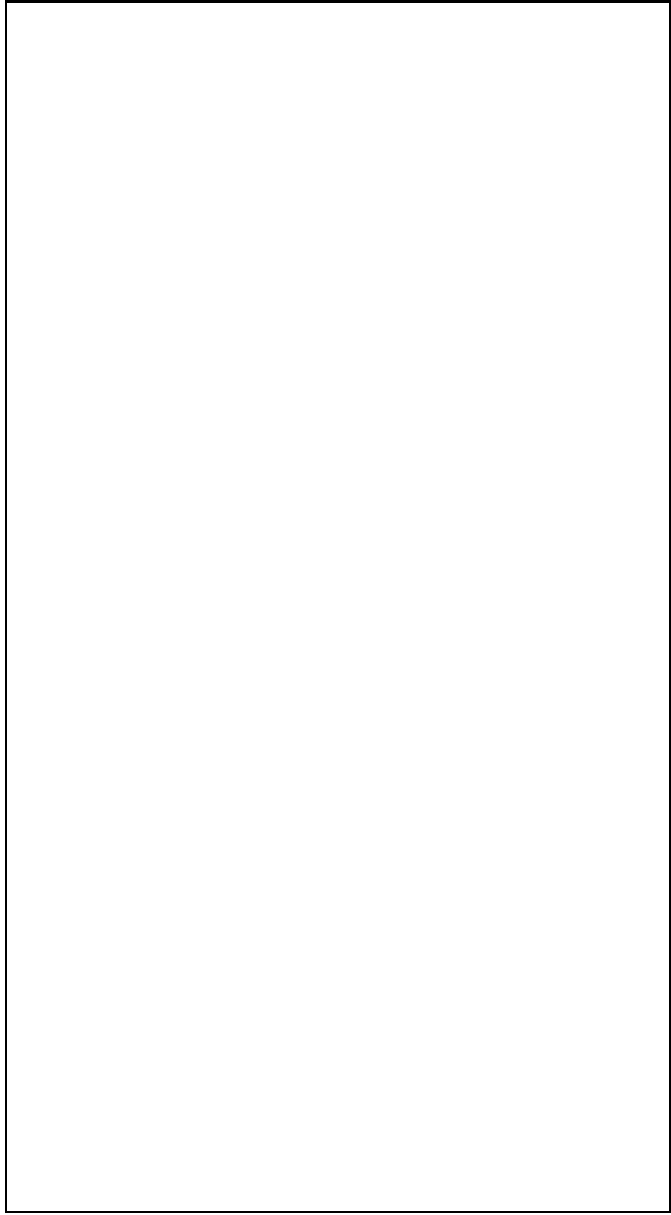


Fig. 2. Time evolution after the end of the burst of: **a** $EW(H\delta)$ (\AA), **b** $(B_J - R_F)$, **c** $(U - 685)$, **d** $(1550 - V)$. The time τ is expressed in Myr. Lines connect models of ellipticals with bursts of $\Delta t = 500$ Myr and $\Delta g = 0.0005$ (empty circles), $\Delta g = 0.005$ (full squares), $\Delta g = 0.025$ (full circles) and $\Delta g = 0.15$ (empty squares)

at least of 0.2 mag. than the average of ellipticals. In both diagrams the colours tend asymptotically to those of the unperturbed elliptical model. Also for these colours the time interval during which they are significantly different from those of the normal elliptical increases with Δg and can last also 1.5 - 2 Gyr as was found for the $H\delta$ line.

The other colours that have been synthesized behave in a similar way. Their sensitivity to the presence of young stars increases with the decrease of the effective wave-

length of the bluer filter; therefore a weak burst affects the $(U-B)$ and $(B-V)$ colours but is unable of modifying substantially for instance the $(R-I)$ colour. In particular the $(1550-V)$ colour index, whose evolution is described by the diagram of Fig. 2d, is able to reveal a star forming activity even if the amount of mass implied is very small (again the horizontal line represents the colour of the unperturbed elliptical).

The general features of the evolution of the index D_{4000} , defined as in Bruzual (1983), are similar to those of the $(B_J - R_F)$ colour; the horizontal line indicates the position of the unperturbed elliptical. Models show that, at the adopted redshift, the following relation exists: $D_{4000} = 0.16 \cdot (B_J - R_F) + 1$.

The $H\delta - (B_J - R_F)$ diagram may give a positive contribution to the understanding of the behaviour of starburst galaxies and particularly of E+A objects. The evolution in this diagram of the model used in Fig. 1 (solid line) and of a second model with $\Delta g = 0.15$ and $\Delta t = 500$ Myr (dashed line) is shown in Fig. 3. The vertical segment and the horizontal line mark respectively the boundary between “blue” and “red” objects and between $H\delta$ -strong ($EW \geq 2.5 \text{ \AA}$ in this case) and $H\delta$ -weak ones. Numbers give the time elapsed since the end of the burst (in Myr). The models of an unperturbed elliptical and that corresponding to the end of the burst are also presented. The discussion of this diagram will be postponed to section 7 where the theoretical data are compared with the observations of three clusters.



Fig. 3. Time evolution of two ellipticals with burst models in the diagram $H\delta$ versus $(B_J - R_F)$. Numbers give the time elapsed since the end of the burst (in 10^6 yr). The empty square marks the position of the unperturbed elliptical model; the two stars represent the positions of the $\tau = 0$ burst models. The vertical segment and the horizontal line mark respectively the division between the “blue”-“red” and the “ $H\delta$ strong”-“ $H\delta$ weak” regions

For a large part of its evolution the equivalent width of $H\delta$ is constant and corresponds to its maximum (Fig. 3). Moreover this maximum is joined to the absence of the $[OII]\lambda 3727$ line, and to colour indexes not too red: from all these features it is easy to recognize when the observed value of $EW(H\delta)$ is at its maximum.

Generally the evolution of the observable quantities depends separately on both Δt and ψ_1/ψ_0 : this is the case, for instance, of $[OII]\lambda 3727$ and other spectral features and all the colours. Only the maximum value of the equivalent width $EW(H\delta)_{\max}$ is correlated with Δg in a simple way. In fact the $EW(H\delta)$ of a single stellar population is high for a long period of time, up to an age of 1.5-2 Gyr. Therefore if Δt is lower than such values all the stellar populations born during the burst contribute in the same way, approximately as if they would have the same age and $EW(H\delta)_{\max}$ is determined only by the total fraction of stars formed during the burst. $EW(H\delta)_{\max}$, which is generally reached about 100 Myr after the end of the burst, is plotted as a function of Δg in Fig. 4 (open circles are of concern at present), for different combinations of Δt and (ψ_1/ψ_0) . Therefore $EW(H\delta)$ can yield an

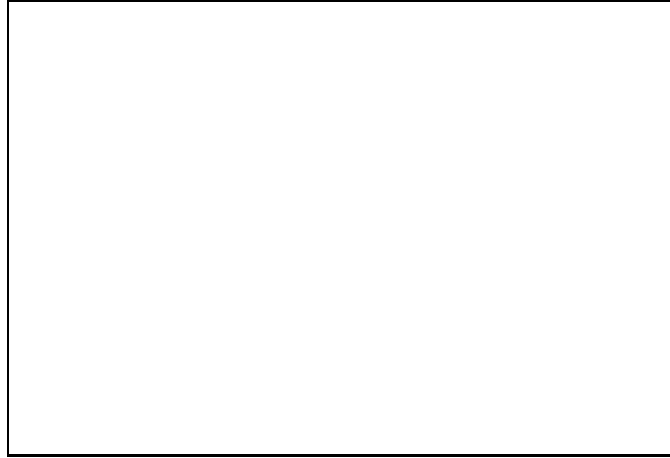


Fig. 4. Dependence of the maximum $EW(H\delta)$ on Δg models of ellipticals with bursts (empty circles) compared to truncated spirals with bursts of different Hubble types (filled circles)

estimation of the amount of mass involved in the burst. Similar conclusions cannot be reached from $EW([OII])$ or $(B_J - R_F)$. $EW(H\delta)_{\max}$ is saturated when $\Delta g \geq 0.20$, that is, when the burst is very strong, it becomes insensitive to the amount of mass involved and in this case only a lower limit to Δg can be set.

Unlike the line flux, the equivalent width of the $[OII]\lambda 3727$ line is not proportional to the number of massive stars formed in the last 10^7 yr. In Fig. 5 $EW([OII])$ is plotted as a function of Δt for different values of the intensity ψ_1/ψ_0 . Provided the intensity is sufficiently high and the length of the burst is large enough, the equiva-

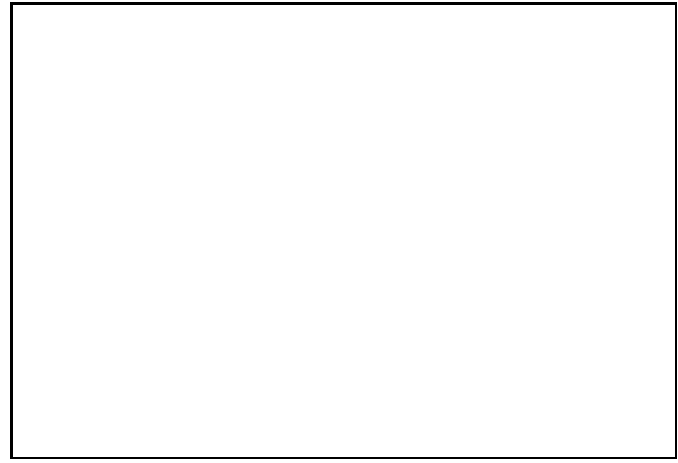


Fig. 5. $EW([OII])$ (\AA) as a function of Δt when the burst is still active ($\tau = 0$). Symbols are: $\psi_1/\psi_0 = 0.001$ (empty circles), $\psi_1/\psi_0 = 0.01$ (full squares), $\psi_1/\psi_0 = 0.05$ (full circles), $\psi_1/\psi_0 = 0.3$ (empty squares). The intervals in Δt are: 1,10,100,500,1000 Myr (1,10,100,260, 400,500,670,850,1000 for the model of highest intensity represented by empty squares)

lent width decreases as the length increases. The reason for this behaviour is that, while the models with the same intensity (same symbol) have the same line flux (the number of ionizing stars being the same), the continuum flux at $\lambda = 3727$ \AA is progressively increasing with Δt , its contribution arising also from stars with lifetime larger than those responsible for the photoionization, and therefore the equivalent width decreases. A similar behaviour is found also in the other emission features, as for instance in $H\delta$ for $\tau = 0$ which, for bursts strong enough, is emission-dominated and in the colours.

5. Bursts in spiral galaxies

When considering bursts in spiral galaxies two possibilities can arise: a) at the end of the burst the SFR can reach again the value typical of its morphological type or b) the star formation is truncated. Case a), referred to as “spirals with bursts”, concerns the situation in which the amount of material involved in the burst is only a small fraction of the available gas or is provided by the environment. In any case it is assumed that the effects of the burst do not hinder any further star formation. Case b) in which, on the contrary, almost all the interstellar gas has been exhausted in the burst, is treated in the truncated spiral models with a burst (TSB).

In order to investigate if strong absorption Balmer lines necessarily imply a burst, models of “truncated spirals” without burst have been also considered. This case would correspond for example to the stripping of the interstellar gas due to the intergalactic medium.

Several types of spirals have been considered; the adopted SFR and metallicity, as functions of the age have

been derived from a standard chemical evolutionary model that includes an inflow and assumes the SFR to be proportional to the gas fraction.

This model provides the SFR and the metallicity as a function of time for galaxies in the type range Sa-Sd. The model parameters for each Hubble type are determined requiring the model SED to reproduce the observed colours and gas fraction of local galaxies. A further model with constant SFR (flat model) has been considered.

5.1. Spirals with bursts

Bursts have been added to models of Sa and Sc galaxies and to the flat model. The explored range of the burst parameters is the same as in the case of ellipticals.

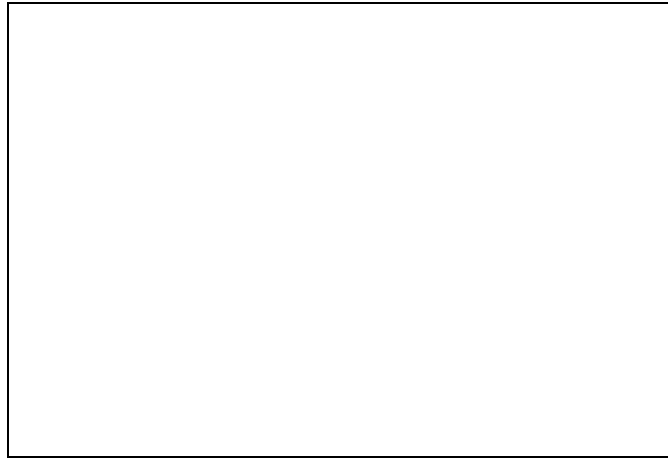


Fig. 6. Time evolution (τ in Myr) of $\text{EW}([\text{OII}])$ (in Å) after the end of the burst in a Sa spiral for $\Delta g = 0.096$ (empty circles and dotted line) and $\Delta g = 0.64$ (filled circles and full line). In these models the SFR is not interrupted at the end of the burst

After the end of the burst such models still present a star formation process and therefore show emission lines, although weaker. The equivalent width of the $[\text{OII}]\lambda 3727$ line is plotted against τ in Fig. 6 for an Sa with a burst in two cases: a burst with $\Delta g = 0.096$ and one with $\Delta g = 0.64$. The equivalent width quickly decreases at the end of the burst due to the reduced SFR, reaching values lower than those characteristic of unperturbed objects of the same morphological type (≈ 10 Å). This ensues from the increase of the continuum around 3727 Å due to the presence of a large number of young stars. $\text{EW}([\text{OII}])$ reaches a minimum for $\tau = 30 - 100$ and afterwards, with a timescale depending on the intensity of the burst, it tends to the unperturbed value. The maximum and the minimum values depend on the intensity, the former increasing and the latter decreasing with ψ_1/ψ_0 .

The $\text{H}\delta$ line, after the end of the burst, is in absorption, even if the star formation is still active and moreover its

intensity is particularly high in the case of strong bursts. The presence of this feature together with $[\text{OII}]\lambda 3727$ in emission can be interpreted in two ways: we are faced with a galaxy having undergone a burst already stopped and with a residual minor SFR or with a post-starburst elliptical in which the burst ended less than 10 Myr ago.

According to these models, spirals with bursts have blue ($B_J - R_F$) colours (< 2 mag) during the whole evolution, with the exception of the very early type spirals with weak bursts or stopped long ago. High values of $H\delta$ can be obtained without truncation, this however is necessary in order to have spectra devoided of emission lines or red colours.

5.2. Truncated spirals with bursts

Different results are obtained if, after the end of the burst, the SFR completely ceases. Smaller percentages of mass involved in the burst are required to reach intense absorption lines compared to the previous case. The minimum Δg required to have $\text{EW}(H\delta) > 3$ Å is however not substantially different. For the rest the results are similar to the case of bursts in ellipticals. The maximum equivalent width of the $H\delta$ line, typically reached at about 100 Myr from the burst end, is independent of the underlying morphological type and depends only on Δg (Fig. 4, filled circles).

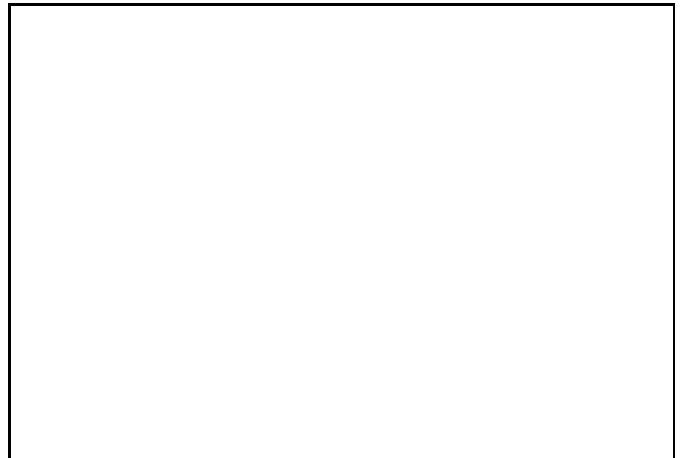


Fig. 7. As Fig. 3 for two Sc galaxies truncated after the burst: $\Delta g = 0.26$ (filled circles) and $\Delta g = 0.026$ (empty circles). The empty and filled squares mark the positions of the unperturbed elliptical and Sc models respectively

The time evolution in the $H\delta - (B_J - R_F)$ diagram shown in Fig. 7, is similar to the corresponding diagram for ellipticals with bursts of Fig. 3. As the evolutionary time scale is the same both in the elliptical and the spiral burst models, the colour of the model is determined only by τ . The only difference is that, in the spiral case, the model

does not relax to the initial values but tends to the colours and equivalent width of the unperturbed elliptical.

5.3. Truncated spirals

Consider the case of a spiral in which the star formation has been completely stopped at some instant. About 10 Myr later the spectrum does not show emission lines at all. The colours evolve towards those of an elliptical with a timescale depending on the morphological type and on the considered colour. Fig. 8a shows the evolution of the $(B_J - R_F)$ colour for different morphological types ($\tau = 0$ marks now the end of the star formation process). A different behaviour is presented by the $(1550 - V)$ (Fig. 8b) which becomes redder than that of the elliptical.

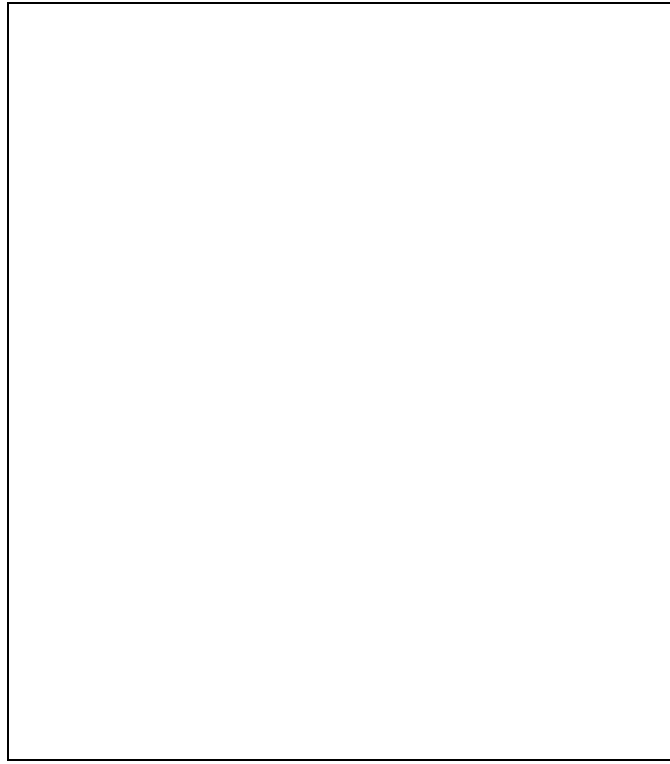


Fig. 8. Truncated spirals without burst: time evolution (τ in Myr) of the colour **a**) $(B_J - R_F)$ and **b**) $(1550 - V)$ after the end of the SF for the Sa (open circles), Sc (filled circles) and constant SFR- model (open squares)

A truncated spiral does not reach $EW(H\delta) > 4.1 \text{ \AA}$, the maximum value increasing with the type (2.3 for Sa, 3.6 for Sc and 4.1 for the flat model). The truncation of the star formation alone therefore is unable to interpret the high equivalent widths observed in distant clusters.

6. A synthetic view

In this section we summarize the main general results derived from our theoretical analysis.

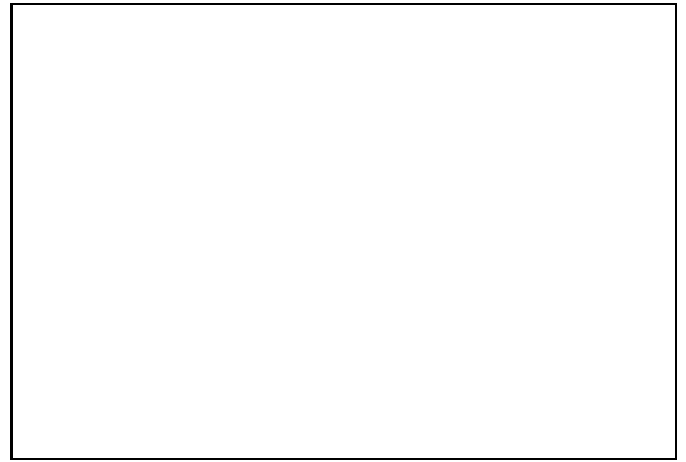


Fig. 9. Post-starburst model spectra: elliptical with a burst (solid line, $\Delta t = 500$ Myr, $\Delta g = 0.15$, $\tau = 500$ Myr); truncated Sa with burst (short dashed line, $\Delta t = 1$ Gyr, $\Delta g = 0.64$, $\tau = 700$ Myr); truncated Sc with burst (long dashed line, $\Delta t = 1$ Gyr, $\Delta g = 0.26$, $\tau = 500$ Myr). The three models have the same $EW(H\delta)$ and the same $(B_J - R_F)$ colour; fluxes are in arbitrary units

1) It has been seen that, concerning the diagrams of Fig. 3 and Fig. 7, the same results are found independently of the original morphological type in which the burst occurs. The question is therefore how to distinguish the original galactic type. In Fig. 9 three post-burst spectra are shown corresponding to different types: E, Sa and Sc. All of them present the same values of $H\delta$ ($\approx 4.5 \text{ \AA}$) and $(B_J - R_F)$ (≈ 2.1). Only for $\lambda < 2000 \text{ \AA}$, do the spirals and the elliptical significantly differ and consequently their $(1550 - V)$ colours would allow their distinction. Spirals are redder since they lack a population of metal-rich, old, hot stars, present in ellipticals. This discrimination can be made only when the bursts are old enough that galaxies are red, otherwise the UV spectral region is dominated by the stars born during the burst. In fact the same models of Fig. 9, viewed only 30 Myr after the burst end, show the same spectral distribution also in the UV region.

2) A current burst or one ended a few Myr ago is undoubtedly witnessed by the presence in the spectrum of an $H\delta$ line in emission or emission-filled and a $[OII]\lambda 3727$ emission line with extremely large equivalent width ($EW \geq 25 \text{ \AA}$). This is however a sufficient but non necessary condition for the presence of a burst.

3) $EW(H\delta)$ reaches its maximum about 100 Myr after the end of the burst and remains almost constant during the whole $H\delta$ -strong phase (Fig. 3 and Fig. 7). Its value depends only on Δg (see Fig. 4). As the period in

which $\text{EW}(\text{H}\delta)$ is approximately at its maximum lasts long enough, the probability of catching an object in this phase is high and this allows the possibility of estimating Δg provided that the following conditions are met: the absence of the $[\text{OII}]\lambda 3727$ emission line, a not too red colour $((\text{B}_J - \text{R}_F) < 2.1)$ and of course an intense $\text{H}\delta$ absorption line. As the maximum of $\text{EW}(\text{H}\delta)$ becomes saturated at $\Delta g \simeq 0.20$, for very strong bursts only a lower limit to Δg can be placed. Due to the steep rise in Fig. 4 the uncertainty in the determination of Δg for relatively weak bursts is large; the accuracy becomes better for stronger bursts.

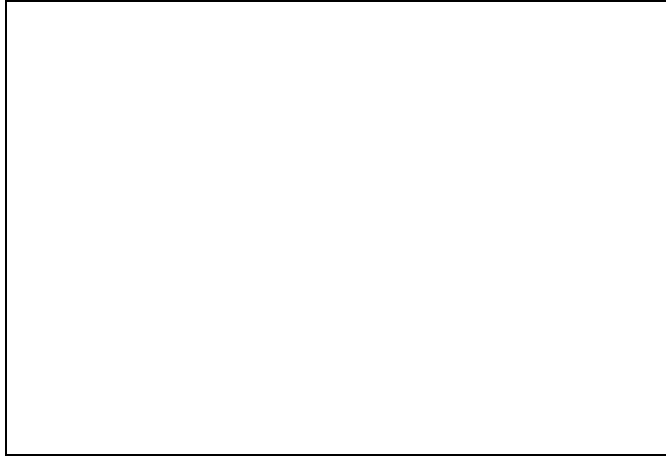


Fig. 10. $\text{EW}(\text{H}\delta)$ - $(\text{B}_J - \text{R}_F)$ diagram divided into zones. Dashed lines delimit the region where the observed $\text{EW}(\text{H}\delta)$ values of spirals from the Kennicutt's sample are placed

4) It is useful to analyze in detail the $\text{H}\delta$ - $(\text{B}_J - \text{R}_F)$ diagram and to subdivide it into several areas, as shown in Fig. 10, according to the partition into blue and red and into $\text{H}\delta$ -strong and $\text{H}\delta$ -weak objects. The horizontal line at $\text{EW}(\text{H}\delta)=1 \text{ \AA}$ together with the other full horizontal line defines the position of the spirals (zone C). Zone F gives the position of red objects with very strong $\text{H}\delta$ lines. As shown in Fig. 3, an elliptical with an intense burst will leave zone A, cross zones B when the burst is still active, C (rapidly in a few million years), D, E or F (phase E+A) and will return again in A. In the case of a truncated spiral with burst, the starting point is located in region C, while the following evolution shows the same features as the ellipticals.

5) The position in the diagram of Fig. 10 allows some delimitation of the parameters of the burst (τ and Δg), as it is clarified in Fig. 11, in which the location of the zones specified in the previous diagram is presented. Physically zone B and zone D are not directly connected, because in most cases a galaxy evolves through B, C and D areas. However the time spent in area C is so short that this phase practically cannot be distinguished in the diagram.

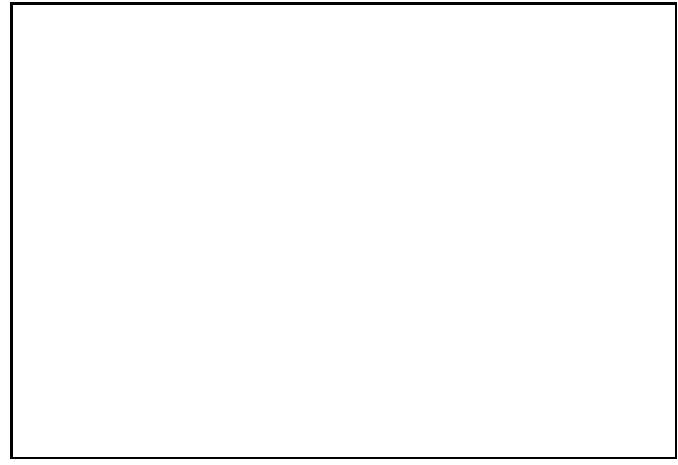


Fig. 11. Location of the regions of Fig. 11 in the parameter space (τ in Myr)

agram. Moreover, due to the limited time resolution of each evolutionary sequence, the boundary between zone B and zone D is uncertain, being located in the interval 4 - 10 Myr. From the same figure we can conclude that, with the exception of the weakest bursts, the evolutionary path crosses the same regions; only the time spent in each area increases with Δg .

Table 2. $(\text{B}_J - \text{R}_F)$ colour ranges corresponding to the various τ during the $\text{H}\delta$ strong phase

τ	$3. < \text{H}\delta < 4.5(\text{\AA})$	$\text{H}\delta > 4.5(\text{\AA})$
10	1.14-1.78	1.32-1.38
30	1.41-1.98	1.54-1.61
100	1.86-2.23	1.77-1.84
500	2.12-2.21	2.03-2.16
1000	2.25-2.33	—
2000	—	—

6) Provided that the $\text{H}\delta$ line is strong, the time elapsed since the end of the burst can be estimated from the $(\text{B}_J - \text{R}_F)$ colour index. This conclusion holds for any kind of underlying galaxy. Table 2 presents such correlation. Any conclusion is of course influenced by the uncertainty affecting the measure of the equivalent width; in the case of strong bursts the determination of τ is more precise. From all the models it turns out that 1.5 Gyr after the end of the burst $\text{EW}(\text{H}\delta)$ is always less than 3 \AA while 700 Myr after $\text{EW}(\text{H}\delta)$ is less than 4.5 \AA . This means that, according to the models, no $\text{H}\delta$ -strong object can be redder than $(\text{B}_J - \text{R}_F) = 2.35$ mag. In the following we shall see that this fact creates some problems in the interpretation of some galaxies in clusters at $z = 0.31$.

Table 3. Minima percentages of galactic mass involved in the burst required to detect such a burst at some point of the evolution

H δ	2.5
R-I	0.5
V-R	0.1
B _J – R _F	0.05
D ₄₀₀₀	0.01
U-685	0.01
H α	0.01
B-V	0.01
U-B	0.001
OII	0.001
1550-V	0.0001

7) Consider an elliptical galaxy to which a burst is added. We determined the minimum Δg required to distinguish such a model from the corresponding unperturbed one, when a given observable is considered and the observational error is taken into account. Table 3 gives such values. In particular $\Delta g = 0.025$ identifies the threshold between H δ -strong and H δ -weak objects. $\Delta g = 0.0005$ separates blue and red objects in the (B_J – R_F) colour. It must be remarked that the evolutionary phases and the time length during which the various quantities show a detectable difference with those of the unperturbed elliptical, depend on the considered observable. Therefore if a given object has a strong H δ line, also the other quantities will show an anomalous behaviour at some moment (not however necessarily the same). In particular this implies that an object in region E of Fig. 10 must have crossed in the past regions B and D. The same conclusion holds if the underlying galaxy is a spiral.

7. Analysis of three clusters at $z = 0.31$

In the following the previous theoretical analysis will be employed to interpret the spectroscopic and photometric data of three clusters at $z = 0.31$ (AC103, AC114 and AC118). CS87 have obtained spectra with a resolution of 4 Å in the spectral region 4750-6750 Å (corresponding to 3625-5150 Å in the rest frame). Moreover they give the colour (B_J – R_F), the apparent magnitude R_F and the equivalent widths in the rest frame of the [OII] $\lambda 3727$ and H δ lines. CS87 confirmed spectroscopically the Butcher-Oemler effect detected photometrically by Couch and Newell (1984). They also found that the red peak of the colour distribution is about 0.2 mag bluer than the expected location of the K-corrected unevolved ellipticals, a fact already noted in the majority of the clusters sampled by Couch and Newell. This shift is larger than the evolutionary correction expected from our models, unless

the time scale of star formation in ellipticals is considerably longer than 1.5 Gyr.

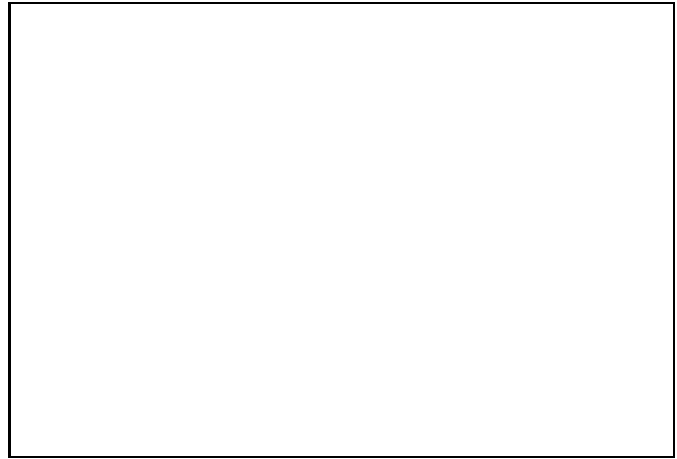


Fig. 12. Observed quantities for the galaxies in the three CS87 clusters (triangles). The equivalent width given is the rest frame value; the colour is reddening corrected. Spiral models (Sa-Sd) are superimposed as filled circles

The equivalent width of [OII] $\lambda 3727$ of all the galaxies with $\text{EW}(\text{[OII]}) > 5$ Å is plotted against (B_J – R_F), corrected for Galactic reddening (Fig. 12); spiral models are also shown. The bluest objects with the strongest emission lines cannot be explained by models of normal galaxies.

Red galaxies have spectra very similar to those of local ellipticals. A fraction of them, however, exhibits an intense absorption H δ line (EW(H δ) = 3 – 5 Å), not found in the spectrum of normal ellipticals. CS87 introduced three classes among blue galaxies: 1) with emission lines and emission-filled Balmer lines; 2) with emission lines and moderate/strong absorption Balmer lines; 3) without emission lines and with strong absorption Balmer lines. All types are present in each cluster, their frequency increases with the class number (from 1 to 3). Most of the blue galaxies do not show emission lines. Only one AGN has been found in AC118; the frequency of such objects in these clusters agrees with that found in local clusters.

CS87 interpreted red H δ -strong objects in terms of starbursts occurred in ellipticals, while spiral progenitors were considered for types 1) and 3). From the analysis of a set of absorption lines (H10(3795 Å), H9(3840 Å), H8(3890 Å), CaIIK(3933 Å), CN(4182 Å) and the G band(4301 Å)), Jablonka & Alloin (1995) concluded that all the red galaxies in the three clusters are elliptical-like objects with traces of star formation 1-5 Gyr ago and that 1/3 of the blue galaxies experienced a recent burst, while the remaining blue objects could be interpreted as early-type spirals.

CESS94 have also obtained further spectroscopy of AC114 and high spatial resolution images with HST. The comparison of the four objects belonging to the two sam-

ples demonstrates the uncertainty in the determination of the equivalent widths. The new spectroscopic data do not introduce any further class, they only increase the number of objects. The HST data of CESS94 provide information about the morphological type and the presence of possible interactions or mergers.

The main HST results for AC114 can be summarized as follows:

- 1) the blue galaxies are mostly disk objects;
- 2) there is a high percentage of interactions/mergers among blue objects;
- 3) H δ -strong red galaxies are apparently isolated ellipticals.

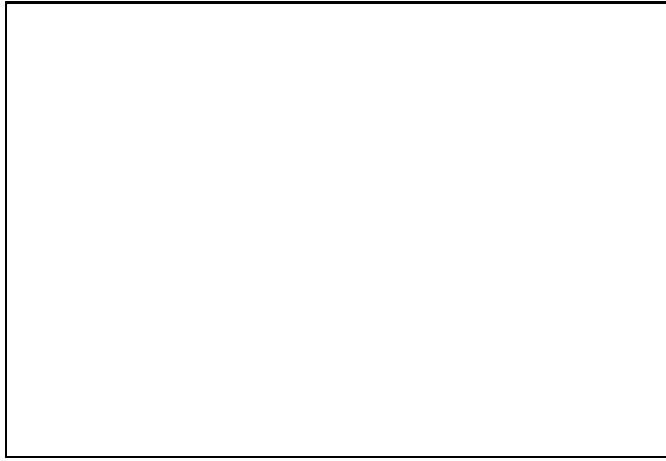


Fig. 13. Observed data for the three clusters placed in the diagram of Fig. 11. Circles are objects without emission lines (empty are blue, filled are red); crosses represent objects with a detectable [OII] $\lambda 3727$ line. From right to left, filled squares show the position in the diagram of the E, Sa, Sb, Sc and Sd models. The dotted lines show the range of EW(H δ) measured from the spectra of the spiral galaxies in Kennicutt's sample

Figure 13 presents the H δ equivalent width and the (B_J - R_F) colour of the objects of the three clusters as well as the subdivision into zones, previously described. Since the errors on the equivalent widths are typically of 1 Å and those on the colour are of 0.1 mag, the position of the objects close to the boundaries need to be considered with some caution. The E, Sa, Sb, Sc and Sd models are also plotted. While the colour range of our models agrees with the models used by CS87 and the observations of Dressler and Gunn (1983), our model EW(H δ) values differ from those of CS87, the latter reaching higher values up to 5 Å and increases steadily with the morphological type. A comparison of these models (Paper II) with the observations of local spirals (Kennicutt 1992) confirms our computed values of EW(H δ) which, for the latest spirals, is the consequence of the emission-filling. When the emission of the ionized gas is neglected our models agree with the results of CS87. Both Kennicutt's observations and our

models show that spiral galaxies present the [OII] $\lambda 3727$ emission line; therefore all the blue objects without emission lines do not have the spectroscopic characteristics of normal spirals. In particular for our spiral models with the adopted age is EW([OII]) > 10 Å. The presence of emission lines indicates the existence of current or recent ($\tau < 10$ Myr) star formation. Their absence implies that in the last 10 Myr the star formation has involved less than 0.001 % of the galactic mass.

We analyze now the whole observational data set by the light of the different kinds of models, starting with ellipticals.

Ellipticals with bursts

Figure 14a shows the same type of diagram of the previous figure in which, instead of the observed data, the models of ellipticals with bursts are located. In this figure models with emission H δ line are not included. These correspond to active bursts begun not long ago: the intensity of the H δ line in emission is large while the underlying continuum is not enhanced yet. Only one object has such a characteristic (#103 di AC114, EW(H δ) = -0.8). The limited number of such objects is amenable to the quickness of the evolution or/and to the fact that burst time lengths are typically longer. Moreover while the star formation is active the H δ remains weak.

Consider in detail the behaviour in the different areas.

- **zone A.** In this region the following models are placed: normal ellipticals, ellipticals with a weak burst, ellipticals with an intense old burst ($\tau \geq 1 - 2$ Gyr). The elliptical model has been computed with an average solar metallicity. Reducing the metal content moves the model horizontally towards bluer colours. Therefore in CS87's sample most objects in zone A could be interpreted as ellipticals of various metallicity.

Ellipticals with a weak burst and ellipticals with an intense old burst can be distinguished from the normal ellipticals on the basis of the (1550 - V) colour, being respectively bluer and redder. Models with emission lines represent ellipticals with a weak burst and $0 < \tau < 10$ Myr. This can be understood remembering that a small amount of newly formed stars is able to give rise to emission lines without modifying the colours (see Table 3). Only one such a case is observed: #12 in AC103.

- **zone B.** In this zone are located galaxies with a current burst consuming more than 0.05 % of the total mass. Models present the [OII] $\lambda 3727$ line and the emission-filled H δ line: this last feature requires that the length of the burst is at least 100 Myr since otherwise the net H δ flux would be in emission. Objects lacking emission lines do not admit any interpretation on the basis of the models: they can be neither starbursts nor post-starbursts. In the former case they should have emission lines, in the latter they would have stronger absorption H δ .

- **zone C.** Normal spirals and ellipticals with bursts just ended ($\tau \approx 10$ Myr) lay in this zone: in the latter the [OII] $\lambda 3727$ line is still present while the emission filling

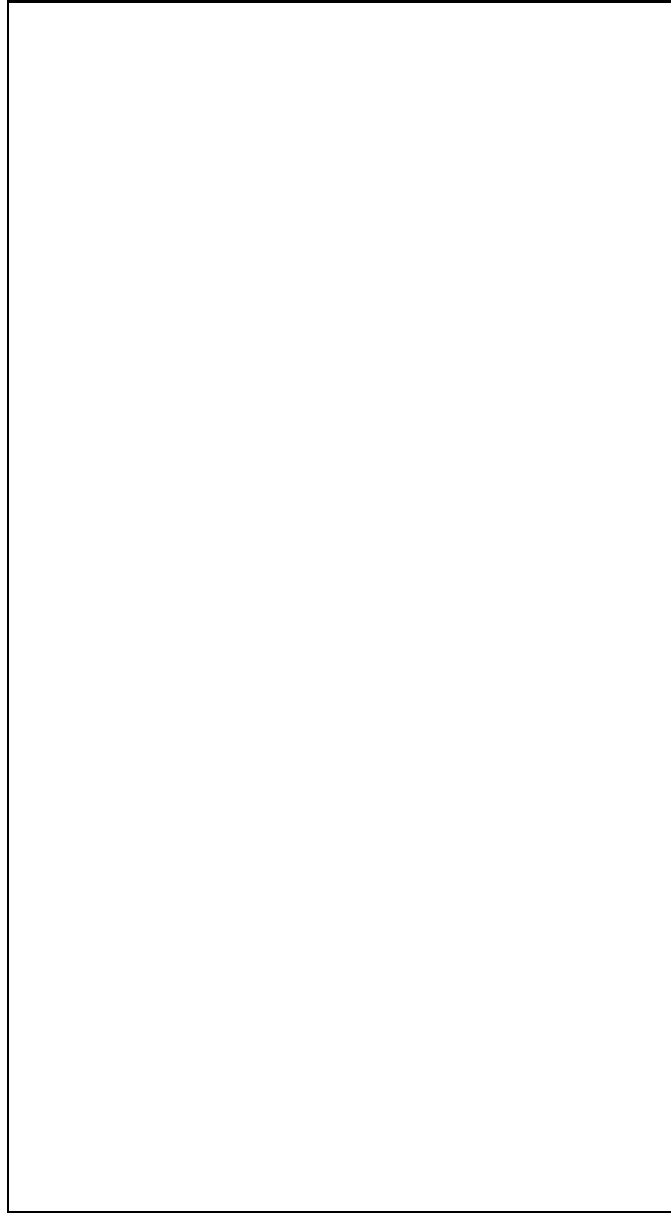


Fig. 14. Results burst models are shown as circles (without emission lines) and crosses (with $\text{EW}([\text{OII}]) > 2 \text{ \AA}$) for the whole burst parameter space investigated. **a)** ellipticals with bursts; **b)** spirals with bursts (without truncation); **c)** truncated spirals with bursts; **d)** truncated spirals without bursts

in the $\text{H}\delta$ line is decreasing. Only one object falls in this region; this however is not ad odds with the number of objects present in zone B, as the evolutionary time in zone C is very short.

- zone D. Models appear with or without emission lines; both type of objects are present among the observed galaxies. In order to reach this area a burst must have occurred with the following characteristics: $\Delta g > 0.025$ and $\tau = 10 - 500 \text{ Myr}$; for models with emission lines the time elapsed since the burst end should not exceed a limit

approximately equal to 30 Myr. It has been shown in Table 2 that in this phase the $(\text{B}_J - \text{R}_F)$ colour is correlated with τ . Objects with $\text{EW}(\text{H}\delta) \geq 7.5 \text{ \AA}$ are not expected due to the saturation of $\text{H}\delta$ with Δg (see Fig. 4) and in fact only one galaxy in the CS87 sample exceeds this limit, within the observational error.

- zone E. In this region the “E+A” galaxies are placed. These are post-starbursts with $\tau = 0.5 - 1.5 \text{ Gyr}$. In this area no object can be found coming directly from zone A: all the $\text{H}\delta$ -strong galaxies must have passed through a blue phase (see Table 3): more precisely it must evolve through the path B, C and D. 1-2 Gyr after the burst end, objects of zone E evolve into region A, as it results from Fig. 3. Models exclude the presence of emission lines in E and in fact no such object is observed.

- zone F. The same conclusions for zone E are valid. One aspect must be stressed: the reddest $((\text{B}_J - \text{R}_F) > 2.3)$ objects with the strongest $\text{H}\delta$ line cannot be interpreted with the present models. Increasing Δg affects the line in the right way but the colour becomes too blue. At least four objects in the considered clusters have such characteristics.

To summarize, the whole observed scenario could be interpreted in terms of starbursts in ellipticals, with the exception of a very limited number of objects, for which a further analysis is desirable.

We extend now our analysis by considering spiral models.

Spirals with bursts. Considering now models of spirals to which a burst is added, in Fig. 14b the $\text{EW}(\text{H}\delta)$ - $(\text{B}_J - \text{R}_F)$ diagram is presented with the usual subdivision into zones. These models assume that the star formation is not interrupted after the end of the burst. They are characterized by emission lines and mostly by blue colours. This type of models is not able to reproduce most of the observed galaxies of Fig. 14a both without emission and E+A, however they could explain $\text{H}\delta$ -strong emission line objects.

Truncated spirals with bursts. This type of models (Fig. 14c) explains the observed diagram as well as ellipticals with bursts: time scales and the covered zones are the same. It has already been shown that, in case of a strong burst, the subsequent evolution is driven by its characteristics and not by the original galaxy type.

Truncated spirals. The maximum $\text{H}\delta$ reached by this type of models is 4 \AA in the case of the latest types; moreover colours are never bluer than 1.7 mag (Fig. 14d). Therefore in order to explain the whole observed diagram, in particular zones B and D, a burst is necessary, being the sole truncation of the star formation insufficient. Only a small fraction of the observations concerning zone D could be interpreted by these models. Truncated spirals cannot interpret also objects in zone B without emission lines because they would evolve above the spiral sequence.

By putting together the results derived from all the kinds of models, the histograms of Δg and τ have been

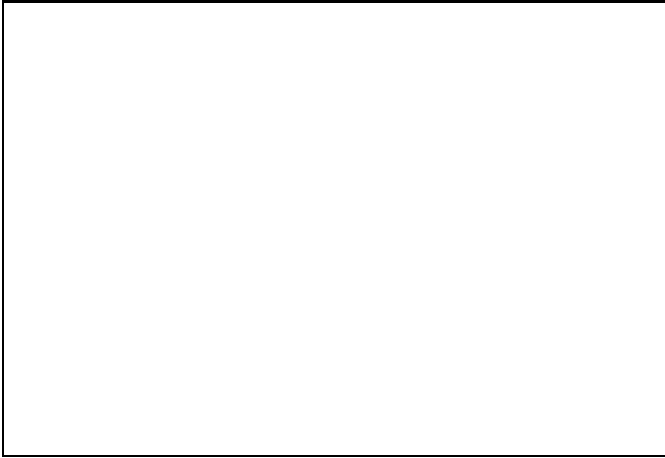


Fig. 15. Distribution in Δg for all the $H\delta$ -strong galaxies with $(B_J - R_F) < 2.3$ mag. Dashed lines show the same distribution for blue objects only. The $EW(H\delta)$ values correspondent to the Δg intervals are also shown

obtained for all the clusters globally, as shown in Fig. 15 and Fig. 16. In the first figure all $H\delta$ -strong objects are included, whose colour is bluer than 2.3 mag. The values of Δg are found from the theoretical relation between $EW(H\delta)$ and Δg of Fig. 4. Let us consider as example a galaxy with $EW(H\delta) = 4$ and $(B_J - R_F) = 2.1$. From Fig. 4 we can conclude that $\Delta g = 0.05 - 0.10$ (therefore the fraction of galactic mass involved is between 5 and 10 %) and from Table 2, second column, a time τ between 100 and 500 Myr is derived.

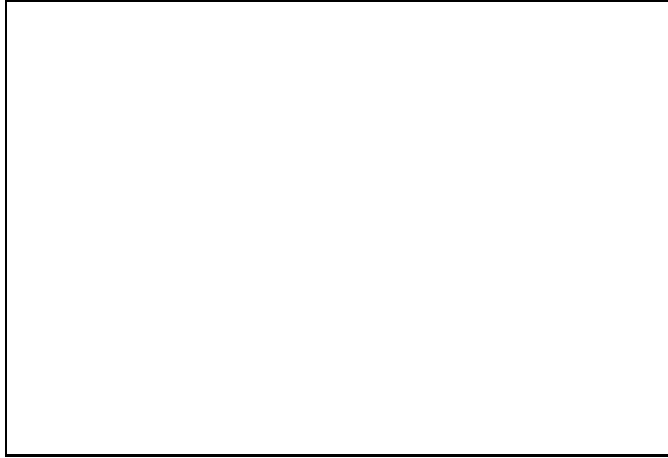


Fig. 16. Distribution of τ for the galaxies in the three clusters: shaded areas correspond to $EW(H\delta) > 4.5$ Å, empty areas to $3 < EW(H\delta) < 4.5$ Å

The distribution of Δg presents two peaks. When however the colour distributions of each Δg interval are analysed, it is found that most of the cases corresponding to

the small- Δg peak are red objects and therefore their $H\delta$ is already decreasing. Neglecting the red objects, the distribution has only the high- Δg peak. We conclude that the bursts identified in the CS87 sample involve in most cases a significant fraction of the galactic mass, of the order of 30 %. We stress that an uncertainty of about 1 Å in $EW(H\delta)$ should always be considered, accounting for the fact that the values obtained depend on the method used to measure the equivalent width: comparing the values of $EW(H\delta)$ obtained from us and from Couch (private communication) of the same spectra, we find differences inside the adopted uncertainty of 1 Å.

The histogram of τ (Fig. 16) is derived from the relation between this timescale and the colour, shown in Table 2 in the case of strong $H\delta$ line. Filled areas refer to objects with $EW(H\delta) > 4.5$ Å, empty areas to $3 < EW(H\delta) < 4.5$ Å. From a pure theoretical point of view one would expect to observe in each interval a number of galaxies proportional to the time interval. This is not the case since an excess of cases with short τ is found; a possible interpretation could be the bias towards current starbursts of the spectroscopic sample, due to the increased luminosity during the burst. Galaxies whose estimated τ is greater than 1 Gyr are rare and this agrees with the relevant decreasing intensity of the $H\delta$ line found in the models.

7.1. Analysis of the cluster Cl1358+6245 at $z = 0.33$

The existence of the Butcher-Oemler effect has been questioned since clusters of galaxies are in most cases selected in the optical and this could provoke a contamination with background and foreground objects, even if the redshift is determined spectroscopically (Koo 1988). A selection based on the luminosity in the X band should avoid this problem; one of the clusters chosen with this criterium is Cl1358+6245 at $z = 0.33$, studied by Fabricant et al. (1991). From the spectra they have derived D_{4000} , $EW([OII])$ and \bar{H} (average value of the equivalent widths of $H\beta$, $H\gamma$ and $H\delta$). Our elliptical model fits well the observations of red passive galaxies (not showing any sign of recent star formation). Models computed for post-starburst galaxies indicate that \bar{H} , to a first approximation, is equal to $EW(H\delta)$, within the errors. The analysis performed for the three AC clusters in terms of $EW(H\delta)$, $EW([OII])$ and $(B_J - R_F)$ has been repeated for this cluster by using D_{4000} instead of the colour, since the equivalence between these two quantities has been previously demonstrated.

From the comparison observations-models for this cluster, we conclude that the same characteristics of the anomalous objects found in the AC clusters are recovered also in Cl1358+6245 even if the selection criteria are completely different.

8. Summary

In this paper a spectrophotometric model has been presented which reproduces the emission of both the stellar and the gaseous component of a galaxy. This model is particularly helpful in understanding phenomena in which a burst of star formation is involved. This is the case of most of the galaxies of the three clusters observed by CS87, in which the presence of a burst is the only way of interpreting the observations.

It has been shown that both the elliptical and the spiral can be the original morphological type, contrary to the findings of CS87. When the spiral type is adopted as the underlying galaxy, in addition to the burst also the truncation is required to give an overall picture of the observations. This however does not exclude that, for a minority of objects, also other mechanisms (truncated spirals, spirals with bursts) can be effective.

The knowledge of the three quantities $\text{EW}([\text{OII}])$, $\text{EW}(\text{H}\delta)$ and the colour ($B_J - R_F$) allows one to determine, in several cases, the burst characteristics. The largest number of constraints is found for the $\text{H}\delta$ -strong objects, in which the time elapsed since the burst end (τ) and the galactic mass fraction of gas exhausted in it (Δg) can be estimated. The histograms of Δg and τ have been obtained; they show that the bursts involve in most cases a significant fraction of the galactic mass (typically 30 % or more).

However the mentioned observed quantities do not uniquely define the original morphological type. Our previous analysis has shown that such a distinction can be obtained by using an UV colour such as ($1550 - V$), which up to now has not been observed in these clusters. Even the direct morphology obtained with HST in principle is not able to identify the original type due to the short dynamical time connected to possible changes in morphology.

Acknowledgements. We would like to thank A. Aragón-Salamanca and H.R. Butcher for useful discussions and comments. We are also grateful to R. Kurucz for sending his new stellar atmosphere models, to M. Auddino who supplied his spiral models and to M. Radovich for running the programme Cloudy for us. We acknowledge the availability of the Kennicutt's galaxy atlas and the Jacoby et al's stellar library from the NDSS-DCA Astronomical Data Center.

References

Aragón-Salamanca A., Ellis E., Sharples R.M., 1991, MNRAS 248, 128

Barbaro G., Olivi F.M., 1986, Spectrophotometric Models of Galaxies. In: Chiosi C., Renzini A. (eds.) Spectral Evolution of Galaxies. Reidel, Dordrecht, p. 283

Barbaro G., Olivi F.M., 1989, ApJ 337, 125

Barbaro G., Poggianti B.M., 1995a, Mem. Soc. Astron. Ital. vol.65 n.3 p.945

Barbaro G., Poggianti B.M., 1996, in preparation (Paper II)

Belloni P., Bruzual A.G., Thimm G.J., Röser H.J., 1995, A&A 297, 61

Bessell, M.S., 1986, PASP 98, 1303

Bessell M.S., Brett, J.M., 1988, PASP 100, 1134

Bruzual A.G., 1983, ApJ 273, 105

Burstein D., Bertola F., Buson L.M., Faber S.M., Lauer T.R., 1988, ApJ 328, 440

Butcher H.R., Oemler A.Jr, 1978, ApJ 219, 18

Butcher H.R., Oemler A.Jr, 1984, ApJ 285, 426

Charlot S., Silk J., 1994, ApJ 432, 453

Couch W.J., Newell E.B., 1980, PASP 92, 746

Couch W.J., Newell E.B., 1984, ApJS 56, 143

Couch W.J., Sharples R.M., 1987, MNRAS 229, 423 (CS87)

Couch W.J., Ellis R.S., Godwin J., Carter D., 1983, MNRAS 205, 1287

Couch W.J., Ellis R.S., Sharples R.M., Smail I., 1994, ApJ 430, 121 (CESS94)

Dressler A., Gunn J.E., 1982, ApJ 263, 533

Dressler A., Gunn J.E., 1983, ApJ 270, 7

Dressler A., Gunn J.E., 1992, ApJS 78, 1

Dressler A., Gunn J.E., Schneider D.P., 1985, ApJ 294, 70

Dressler A., Oemler A.Jr, Butcher H.R., Gunn J.E., 1994, ApJ 430, 107

Ellis R.S., Couch W.J., MacLaren I., Koo D.C., 1985, MNRAS 217, 265

Fabricant D.G., McClintock J.E., Bautz M.W., 1991, ApJ 381, 33

Ferland G.J., 1991, Hazy: a brief introduction to Cloudy 80.06, OSU Astronomy Department - Internal Report 91-01

Gunn J.E., Dressler A., 1988, Cluster Galaxies at High Redshift. In: Kron R.G., Renzini A. (eds.) Towards Understanding Galaxies at Large Redshift. Kluwer, Dordrecht, p.227

Jablonka P., Alloin D., 1995, A&A 298, 361

Jablonka P., Alloin D., Bica E., 1990, A&A 235, 22

Jacoby G.H., Hunter D.A., Christian C.A., 1984, ApJS 56, 257

Kennicutt R.C.Jr, 1992, ApJS 79, 255

Koo D.C., 1988, A Deep Redshift Survey of Field Galaxies. In: Kron R.G., Renzini A. (eds.) Towards Understanding Galaxies at Large Redshift. Kluwer, Dordrecht, p.209

Kurucz R., 1993, CD-Rom n.13, version 22/10/93

Lançon A., Rocca-Volmerange B., 1992, A&AS 96, 593 (LRV)

Lavery R.J., Henry J.P., 1986, ApJ 304, L5

Lavery R.J., Henry J.P., 1988, ApJ 330, 596

Lavery R.J., Henry J.P., 1994, ApJ 426, 524

Lilly S.J., 1987, MNRAS 229, 573

MacLaren I., Ellis R.S., Couch W.J., 1988, MNRAS 230, 249

Mellier Y., Soucail G., Fort B., Mathez G., 1988, A&A 199, 13

Newberry M.V., Boruson T.A., Kirshner R.P., 1990, ApJ 350, 585

Oemler A.Jr, Dressler A., Butcher H.R., 1995, ApJ in press

Pickles A.J., van der Kruit P.C., 1988, Interpreting Integrated Spectra. In: Kron R.G., Renzini A. (eds.) Towards Understanding Galaxies at Large Redshift. Kluwer, Dordrecht, p.29

Pickles A.J., van der Kruit P.C., 1991, A&AS 91, 1

Poggianti B.M., Barbaro G., 1994, Butcher-Oemler Effect: Bursts or Truncated Star Formation? In: Durret F., Mazure A., Tran Thanh Van J. (eds.) Clusters of Galaxies. Editions Frontières, Gif-sur-Yvette Cedex, p.419

Poggianti B.M., Barbaro G., 1995, Mem. Soc. Astron. Ital. vol.65 n.3 p.953

Rakos K.D., Schombert J.M., 1995, ApJ 439, 47
Schneider D.P., Gunn J.E., Hoesel J.G., 1983, ApJ 264, 337
Soucail G., Mellier Y., Fort B., Cailloux M., 1988, A&AS 73,
471
Stasinska G., 1990, A&AS 83, 501
Wirth G.D., Koo D.C., Kron R.G., 1994, ApJ 435, L105